

DUST ACCUMULATION FROM MEDA MEASUREMENTS AT JEZERO CRATER, MARS. A. Vicente-Retortillo¹, M. T. Lemmon², G. M. Martinez³, D. Toledo⁴, V. Apestigue⁴, I. Arruego⁴, J. A. Rodriguez-Manfredi¹, ¹Centro de Astrobiología (CSIC-INTA), Madrid, Spain (adevicente@cab.inta-csic.es), ²Space Science Institute, Boulder, CO, USA, ³Lunar and Planetary Institute, USRA, Houston, TX, USA, ⁴Instituto Nacional de Técnica Aeroespacial (INTA), Madrid, Spain.

Introduction: Dust is present in the Martian atmosphere throughout the year, posing challenges to the exploration of the planet. Dust affects the performance and lifetime of infrastructure, and this is particularly important for solar-powered missions [1-4]. In addition, the combined analysis of the temporal evolution of dust accumulation and contemporaneous environmental measurements provides insights into dust lifting mechanisms and dust accumulation rates [5].

Since February 2021, the Mars Environmental Dynamics Analyzer (MEDA) [6], onboard the Mars 2020 Perseverance rover, has been monitoring changes in atmospheric variables (such as solar radiation, pressure and wind) [7,8] and surface properties (albedo and thermal inertia) [9,10]. Solar radiation and dust abundance measurements allow the analysis of the temporal evolution of dust accumulation [11].

Observations and methodology: MEDA contains a Radiation and Dust Sensor (RDS), which is located on the rover deck. The RDS consists of two sets of 8 photodetectors, one of them of them (TOP) pointing at the zenith in several bands between ultraviolet and near infrared wavelengths, and the other (LAT) pointing sideways with an elevation of 20° (except for channel LAT8). These detectors are distributed around a sky-facing camera, Skycam [6,12]. On the other hand, Mars 2020 is equipped with Mastcam-Z [13], which can also measure dust opacity.

The methodology employed in this work relies on the one developed for the analysis and correction of the Mars Science Laboratory REMS UV measurements [5,14], but differences between both instruments allow some simplifications for MEDA. Here, we use measurements of solar radiation acquired by the RDS TOP7 channel, which measures incoming radiation between 190 and 1100 nm with a hemispheric field of view, to analyze dust accumulation on the detector's window. The effect of the dust suspended in the atmosphere is considered using Mastcam-Z opacities at 880 nm and the radiative transfer model COMIMART [15]. In addition, the methodology considers rover tilt and orientation and sensor's angular response.

We quantify the effect of accumulated dust by means of the dust correction factor (DCF), which indicates the fraction of the incoming radiation at the surface that reaches the photodiode through the dust

accumulated on the window, normalized to the first sol for which the DCF is retrieved.

Results:

Temporal evolution of the DCF. Figure 1 shows the dust correction factor (red) and the dust opacity (green) during the first 578 sols (0.86 Mars years) of the mission. After sol 475, accumulated dust attenuates between 15% and 20% of the incoming solar radiation. A significant increase in dust accumulation is observed during the period with atmospheric opacity above 1; in contrast, there is little to no net dust accumulation outside that temporal window.

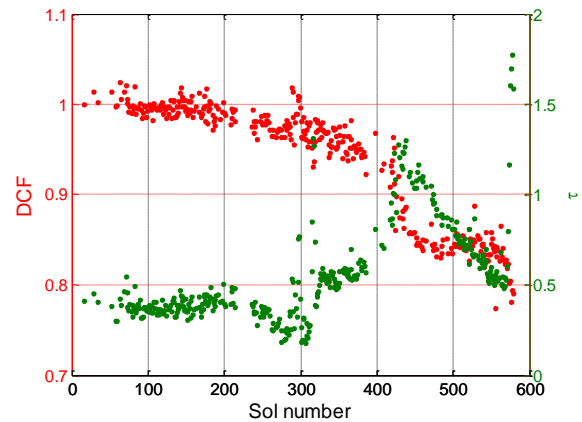


Figure 1. Dust correction factor (red) and dust opacity (green) during the first 578 sols of the Mars 2020 mission.

Between sols 313 and 318, a regional dust storm affected Jezero crater, with peak opacities above 1. Mars 2020 observations indicate an extraordinarily high dust lifting activity at the location of Perseverance during this storm [9,16], but the DCF did not show large changes during this period. This could be attributed to the fact that there was little dust accumulation before the storm, and therefore even the removal of all of the accumulated dust would not lead to a clear increase of the DCF, such as the ones observed by Spirit, where the DCF increased more than 0.4 around sol 420 [2].

Estimation of dust lifting and deposition rates. We have run a model to simulate dust accumulation using dust opacity observations and tuning the dust removal and deposition rates. Figure 2 compares the DCF observations with a model simulation that fits well the data. This good fit is achieved assuming that there is an

additional dust deposition of 0.2% of the total column dust per sol, and that there is a dust removal of 0.49% per sol [11].

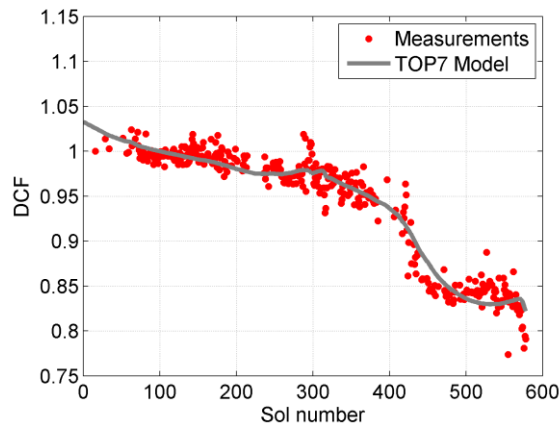


Figure 2. Simulated evolution of dust accumulation (gray; dust deposition and lifting rates of $0.002\tau/\text{sol}$ and $0.0049/\text{sol}$, respectively), compared to the observed DCF (red).

Comparison with other instruments and missions.

Figure 3 shows a model simulation of the DCF using Skycam observations (which are normalized to the fit). Both TOP7 and Skycam DCF show a slow decrease during the first 300 sols and a rapid decrease during the period of enhanced opacity. The most notorious difference is the occurrence of net dust removal between sols 311 and 320, attributed to the dust storm.

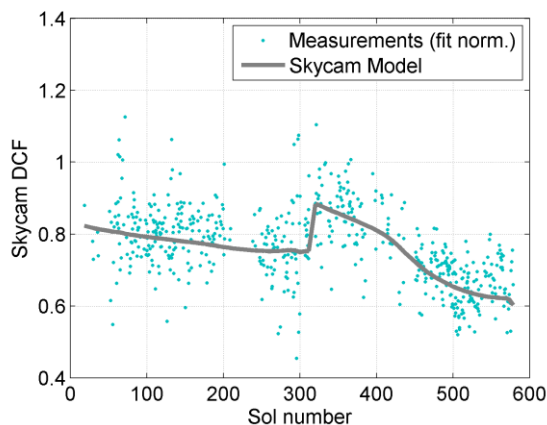


Figure 3. Simulated evolution of dust accumulation on the Skycam window (gray), and individual observations (dark cyan) normalized to the fit.

This difference could be attributed to differences in dust removal thresholds on both surfaces or to a larger amount of pre-storm accumulated dust on the Skycam window. This second factor is supported by the model results: The model runs determine the initial dust accumulation that optimizes the fit; considering the potential initial dust accumulation, attenuation by

accumulated dust on the TOP7 photodiode would be approximately half of that on the Skycam window.

Finally, we compare the DCF from Mars 2020 with those of other missions. In absence of dust removal, dust deposition rates on solar panels are around $0.2\%/sol$ for Spirit, Opportunity or InSight [17]. At this rate, the DCF on sol 500 would be 0.37, which is significantly lower than the observed value of 0.85. This indicates that there is a persistent dust removal mechanism at Jezero crater that mitigates significantly the effect of dust accumulation.

In addition, the comparison corroborates the need of a daily dust removal rate when modeling the DCF from MEDA observations. The difference with previous missions could be attributed to the time of the year and atmospheric conditions: dust opacities remained below 0.5 during the first 300 sols of the mission, and there is vast evidence of frequent dust lifting events around the rover [8, 9, 16, 18, 19], leading to small net dust accumulation rates.

Acknowledgments: This research has been funded by the Comunidad de Madrid Project S2018/NMT-4291 (TEC2SPACE-CM) and by the Spanish Ministry of Science and Innovation (MCIN) project RTI2018-098728-B-C31. MEDA measurements are stored in the NASA PDS (https://pds-atmospheres.nmsu.edu/data_and_services/atmospheres_data/PERSEVERANCE/meda.html).

References: [1] Crisp, D. et al. (2004) *Acta Astronautica*, 54(2), 83-101. [2] Stella, P. M. and Herman, J. A. (2010) *PVSC*, 35th IEEE, 2631–2635. [3] Drube, L. et al. (2010) *JGR Planets*, 115 (E5). [4] Lorenz, R. D. et al. (2020) *Earth and Space Science*, 7(5), e2019EA000992. [5] Vicente-Retortillo, Á. et al. (2018) *Scientific Reports*, 8(1), 1-8. [6] Rodriguez-Manfredi, J. A. et al. (2021) *Space Science Reviews*, 217(3), 1-86. [7] Rodriguez-Manfredi, J.A. et al. *Nature Geoscience* (accepted). [8] Newman et al. (2022) *Science Advances*, 8(21), eabn3783. [9] Vicente-Retortillo, A. et al. *JGR Planets* (under review) [10] Martinez, G.M. et al. *JGR Planets* (under review). [11] Vicente-Retortillo et al. *GRL* (in prep.) [12] Apéstigue, V. et al. (2022) *Sensors*, 22(8), 2907. [13] Bell, J.F. et al. (2021), *Space Science Reviews*, 217(1), 1-40. [14] Vicente-Retortillo, A. et al. (2020) *Space Science Reviews*, 216(5), 1-19. [15] Vicente-Retortillo et al. (2015) *Journal of Space Weather and Space Climate* 5, A33. [16] Lemmon, M.T. et al. (2022) *GRL*, 49(17), e2022GL100126. [17] Lorenz, R.D. et al. (2021) *Planetary and Space Science* 207, 105337. [18] Hueso, R. et al. *JGR Planets* (accepted) [19] Toledo, D. et al. *JGR Planets* (accepted).